Thickness dependence of the efficiency of polymer

Lenes, M.; Koster, L. J. A.; Mihailetchi, V. D.; Blom, P. W. M.

Published in:
Applied Physics Letters

DOI:
10.1063/1.2211189

Publication date:
2006

Thickness dependence of the efficiency of polymer:fullerene bulk heterojunction solar cells

M. Lenes[a] and L. J. A. Koster
Molecular Electronics, Materials Science Centre[Plus], University of Groningen, Nijenborgh 4, 9747 AG Groningen, The Netherlands and Dutch Polymer Institute, P.O. Box 902, 5600 AX Eindhoven, The Netherlands

V. D. Mihailetchi and P. W. M. Blom
Molecular Electronics, Materials Science Centre[Plus], University of Groningen, Nijenborgh 4, 9747 AG Groningen, The Netherlands

(Received 22 December 2005; accepted 26 April 2006; published online 12 June 2006)

We study the thickness dependence of the performance of bulk heterojunction solar cells based on poly[2-methoxy-5-(3′,7′-dimethyloctyloxy)-1,4-phenylenevinylene] as electron donor and [6,6]-phenyl C_{61} butyric acid methyl ester as electron acceptor. Typically, these devices have an active layer thickness of 100 nm at which only 60% of the incoming light is absorbed. Increasing device thickness results in a lower overall power conversion efficiency, mainly due to a lowering of the fill factor. We demonstrate that the decrease in fill factor and hence device efficiency is due to a combination of charge recombination and space-charge effects. © *2006 American Institute of Physics*. [DOI: 10.1063/1.2211189]

Organic photovoltaic devices based on blends of conjugated polymers and fullerene derivatives are considered as promising candidates for low-cost, flexible, and large area photovoltaic devices. One of the most studied systems in this field consists of poly[2-methoxy-5-(3′,7′-dimethyloctyloxy)-1,4-phenylenevinylene] (MDMO-PPV) as electron donor and [6,6]-phenyl C_{61} butyric acid methyl ester (PCBM) as electron acceptor achieving power conversion efficiencies of up to 2.5% under AM1.5 illumination.[1] A striking feature of these types of solar cells is that at the optimal device thickness of typically 100 nm only 60% of the incident light is absorbed.[2] It is evident that the absorption can be enhanced by increasing the thickness of the active layer. However, in spite of an increased absorption, the overall power conversion efficiency does not improve when increasing the device thickness beyond 100 nm. This has been attributed to an increasing series resistance,[3,4] although its physical meaning is not clear for solar cells where charge carriers are generated throughout the device. Furthermore, a thickness increase is expected to give rise to an enhanced charge recombination because of an increase in carrier drift length.[3,5,6] From a device point of view the reduced performance with increasing thickness mainly originates from a decrease of the fill factor. In this study the origin of this decreasing fill factor is investigated.

It has been shown that for devices with a large difference in electron and hole mobilities a space-charge limited (SCL) photocurrent occurs at high intensity due to an unbalanced charge transport.[7,8] Such a SCL photocurrent can be described by the following relation:

$$J_{\mathrm{ph}} \leqslant (qG)^{0.75}\left(\frac{9}{8}\varepsilon_0\varepsilon_r\mu_h\right)^{0.25}\sqrt{V}, \tag{1}$$

where G is the generation rate of free carriers and μ is the mobility of the slowest carrier, holes in this case. Thus, a pure SCL photocurrent is characterized by a square-root dependence on voltage and a three quarter dependence on intensity and, taking into account the dark current of a device, will have a maximum fill factor of 42% opposed to ~60% for standard MDMO-PPV:PCBM devices. Note that Eq. (1) does not depend on device thickness. For non-space-charge limited devices, however, as is the case for standard MDMO-PPV:PCBM solar cells, the photocurrent density at short circuit and reverse bias is closely approximated by $J=qG(E,T)L$, with q the elementary charge, $G(E,T)$ the field and temperature generation rates of free carriers, and L the sample thickness.[9] Consequently, in this case increasing the active layer thickness will generally result in a higher photocurrent due to an enhanced absorption. As a result, with increasing active layer thickness at some point the photocurrent will reach the (thickness independent) space-charge limit given by Eq. (1) and a transition will occur from a non-SCL to a SCL device. Such a transition will lead to a strong decrease of the fill factor, even when charge recombination does not play a role.

In this study solar cells are made of a blend of MDMO:PPV and PCBM in a 1:4 weight ratio. The blend is sandwiched in between a hole-conducting layer of poly(3,4 ethylenedioxythiophene)/poly(styrenesulfonate) (PEDOT:PSS), and an evaporated lithium fluoride (LiF) (1 nm)/aluminum (100 nm) top electrode. Varying the spin procedure resulted in active layer thicknesses ranging from 128 to 368 nm. After fabrication the current-voltage characteristics of these devices were measured in nitrogen atmosphere under illumination of a white light halogen lamp calibrated by a silicon photodiode. To obtain light intensity dependent measurements, a set of neutral density filters was used, yielding an intensity variation of two orders of magnitude. Figure 1 shows the open circuit voltage (V_{oc}), short circuit current (J_{sc}), fill factor (FF), and overall power efficiency (η) of the created devices at approximately 1 kW/m^2 intensity. When increasing the active layer thickness the increase in short circuit current is canceled by a decrease in the fill factor and hence the overall power conversion efficiency

[a]Electronic mail: m.lenes@rug.nl

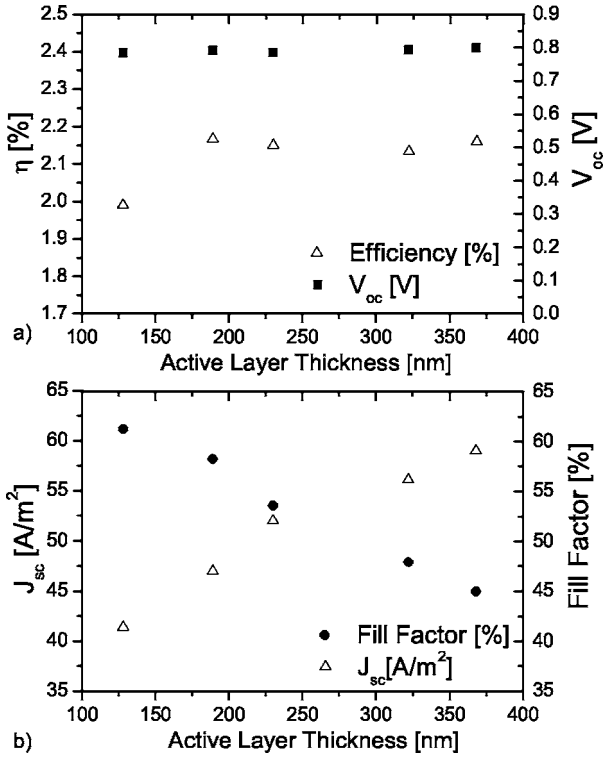

FIG. 1. Overall power conversion efficiency (η), open circuit voltage (V_{oc}), short circuit current (J_{sc}), and fill factor (FF) as a function of active layer thickness under 1 kW/m^2 illumination.

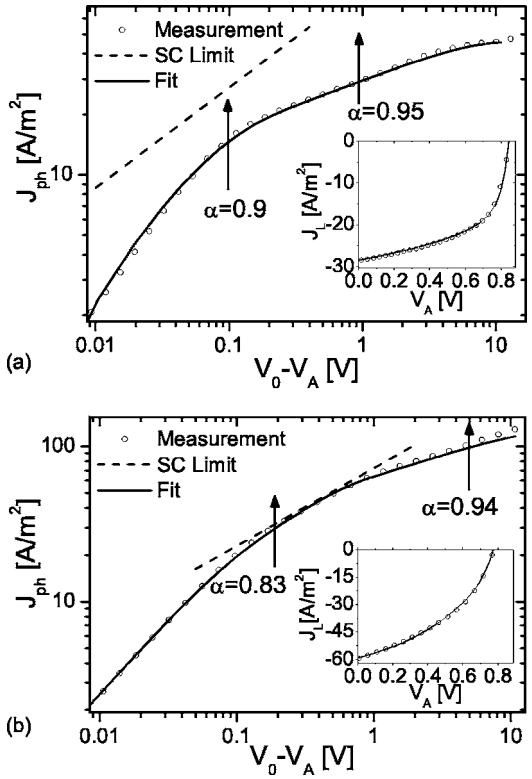

FIG. 2. Experimental photocurrent density J_{ph} as a function of effective applied voltage V_0-V_A under 1 kW/m^2 illumination for a device consisting of a 128 nm active layer (a) and 368 nm active layer (b). Circles indicate experimental data, solid line indicates fits of the photocurrent, and the dashed line indicatess the predicted space-charge limit using Eq. (1). The arrows indicate fits of the intensity dependence $J_{ph} \propto I^{\alpha}$. Inset: current under illumination J_L vs applied voltage V_A.

does not increase. To explain this behavior photocurrents of devices with a thin (128 nm) and a thick (368 nm) active layer have been studied in more detail, including their illumination intensity dependence. Figure 2 shows the photocurrent density $J_{ph}=J_L-J_D$, where J_L and J_D are the current density under illumination and in dark, respectively, as a function of effective applied voltage V_0-V_A for both devices. Here V_0 is the compensation voltage defined as J_{ph} $(V_0)=0$ and V_A is the applied bias. Also shown is the predicted space-charge limit using $\mu_h=3\times10^{-8}$ m^2/V s and $G=1.9\times10^{27}$ and 0.9×10^{27} m^{-3} s^{-1} for both devices. In the case of the 128 nm device the photocurrent is still below the space-charge limit and two regimes can be recognized;[9] for voltages close to V_0 the photocurrent scales linearly with effective applied voltage due to a competition between drift and diffusion currents. As mentioned above, with increasing applied voltage ($V_0-V_A>0.1$ V) the photocurrent saturates to $J_{ph}=qG(E,T)L$. For the 368 nm device, however, the photocurrent intersects the predicted space-charge limit and now three regimes appear. Again the photocurrent is linear for small applied voltages ($V_0-V_A<0.1$ V). In the second regime (0.3 V$<V_0-V_A<0.7$ V) the photocurrent now shows the typical square-root dependence of a SCL photocurrent followed by a saturation of the photocurrent ($V_0-V_A>0.7$ V). It is evident that the occurrence of the space-charge regime will have a strong effect on the fill factor of the 368 nm device. In order to further confirm the built-up of space charge in the thick devices we investigated the dependence of the photocurrent J_{ph} on light intensity I, characterized by $J_{ph} \propto I^{\alpha}$. In Fig. 2 the coefficient α is given for various effective voltages. For the thin device α ranges from 0.9 in the linear regime to 0.95 in the saturated regime indicating that almost no space-charge effects occur.[10] For the thick device $\alpha=0.83$ at $V_0-V_A=0.2$ V, approaching the theoretical value of $\frac{3}{4}$ for the pure space-charge dominated regime.

As a next step a numerical model[11] which includes drift and diffusion of charge carriers, the effect of space-charge on the electric field, bimolecular recombination, and a field and temperature dependent generation rates of free charge carriers is applied to gain insight into the loss mechanisms in thin and thick solar cells. Since charge carrier densities in MDMO-PPV:PCBM solar cells are typically in the order of 10^{21} m^{-3} and at these densities no significant effect on charge carrier mobility is expected we assume a constant charge carrier mobility.[11,12] Figure 2 shows the fits of the current-voltage characteristics of the thin and thick devices. In Fig. 3 the calculated potential through the 368 nm device in the dark and under illumination is shown. As expected for a space-charge limited device the electric field near the anode is increased due to a buildup of holes and the electric field near the near the cathode is decreased. The simulations allow us to disentangle the various loss mechanism at maximum power point (MPP) and short circuit, as shown in Table I. First, the average dissociation rate $\langle P \rangle$ decreases for thicker devices as a result of the lower electric field in the device. At the MPP the dissociation efficiency drops from 51.5% for the 128 nm device to 40% for the 368 nm thick solar cell. Furthermore, the amount of carriers lost due to recombination at MPP and short circuit is also shown. The recombination losses at MPP increase from 14% for the thin device to 35% for the thick device. This shows that next to space-charge formation also the reduced dissociation effi-

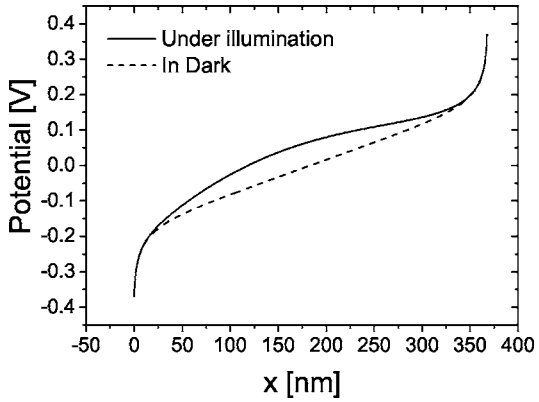

FIG. 3. Simulation of the potential (anode left, cathode right) through the 368 nm device at maximum power point under illumination (solid line) and in dark (dashed line) indicating the effects of space charge.

ciency and increased recombination losses play a significant role in thick polymer solar cells. It should be noted that it is not possible to exactly quantify the losses due to these various processes individually, since they are all interrelated. For example, due to space-charge formation the electric field in a large part of the device is reduced, leading also to a reduced dissociation and to an increase of the charge carrier transit times. This in turn will lead to an increase of the charge recombination. In that sense, the increase of the transit time due to an increased thickness of the active layer is not only due to an increase in the distance carriers need to traverse, but is further amplified by space-charge formation.

TABLE I. An overview of voltage, current density, average dissociation probability, and relative number of free carriers lost due to recombination at short circuit (sc) and maximum power point (MPP) for a 128 and a 368 nm device.

	V (V)	J_L (A/m^2)	$\langle P \rangle$ (%)	Recombination losses (%)
128 nm device	$V_{sc}=0$	29.0	61	2
	$V_{MPP}=0.653$	19.5	52	14
368 nm device	$V_{sc}=0$	59.8	45	9
	$V_{MPP}=0.50$	37.7	40	35

To conclude, increasing the active layer thickness of MDMO-PPV:PCBM bulk heterojunction solar cells does not result in a higher power conversion efficiency because the increase in short circuit current is canceled by a decrease in the fill factor. It has been shown that this decrease in the fill factor originates from the occurrence of a space-charge limited regime in the photocurrent. Secondly, charge recombination is increased in thicker samples, both by space charge effects and by an increase in the distance carriers need to traverse. The way to overcome this limitation is to enhance the transport of the slowest charge carriers, in this case the photogenerated holes in the MDMO-PPV.

The work of the two authors (M.L.) and (L.J.A.K.) forms part of the research program of the Dutch Polymer Institute (Nos. 524 and 323).

[1] C. J. Brabec, N. S. Sariciftci, and J. C. Hummelen, Adv. Funct. Mater. **11**, 15 (2001).
[2] S. E. Shaheen, C. J. Brabec, N. S. Sariciftci, F. Padinger, T. Fromherz, and J. C. Hummelen, Appl. Phys. Lett. **78**, 841 (2001).
[3] P. Schilinsky, C. Waldauf, J. Hauch, and C. J. Brabec, J. Appl. Phys. **95**, 2816 (2004).
[4] I. Riedel, J. Parisi, V. Dyakonov, L. Lutsen, D. Vanderzande, and C. J. Brabec, Adv. Funct. Mater. **14**, 38 (2004).
[5] I. Riedel and V. Dyakonov, Phys. Status Solidi A **201**, 1332 (2004).
[6] W. Ma, C. Yang, X. Gong, K. Lee, and A. J. Heeger, Adv. Funct. Mater. **15**, 1617 (2005).
[7] A. M. Goodman and A. Rose, J. Appl. Phys. **42**, 2823 (1971).
[8] V. D. Mihailetchi, J. Wildeman, and P. W. M. Blom, Phys. Rev. Lett. **94**, 126602 (2005).
[9] V. D. Mihailetchi, L. J. A. Koster, J. C. Hummelen, and P. W. M. Blom, Phys. Rev. Lett. **93**, 216601 (2004).
[10] L. J. A. Koster, V. D. Mihailetchi, H. Xie, and P. W. M. Blom, Appl. Phys. Lett. **87**, 203502 (2005).
[11] L. J. A. Koster, E. C. P. Smits, V. D. Mihailetchi, and P. W. M. Blom, Phys. Rev. B **72**, 085205 (2005).
[12] C. Tanase, P. W. M. Blom, and D. M. de Leeuw, Phys. Rev. B **70**, 193202 (2004).